Environmental Pollution 317 (2023) 120811

Contents lists available at ScienceDirect

Environmental Pollution

journal homepage: www.elsevier.com/locate/envpol

Dydrogesterone disrupts lipid metabolism in zebrafish brain: A study based on metabolomics and Fourier transform infrared spectroscopy☆

Yu-Xia Jiang [a,b,c], Wen-Jun Shi [a,*], Li-Xin Hu [a], Dong-Dong Ma [a], Hui Zhang [d], Choon Nam Ong [e], Guang-Guo Ying [a]

[a] SCNU Environmental Research Institute, Guangdong Provincial Key Laboratory of Chemical Pollution and Environmental Safety & MOE Key Laboratory of Theoretical Chemistry of Environment, South China Normal University, Guangzhou 510006, China
[b] South China Institute of Environmental Sciences, Ministry of Ecology and Environment, Guangzhou 510535, China
[c] State Key Laboratory of Organic Geochemistry, Guangzhou Institute of Geochemistry, Chinese Academy of Sciences, Guangzhou 510640, China
[d] NUS Environmental Research Institute, National University of Singapore, Singapore, 117411
[e] School of Public Health, National University of Singapore, Singapore, 117547

ARTICLE INFO

Keywords:
Dydrogesterone
Zebrafish
Brain
Metabolomics
FTIR
Lipid metabolism

ABSTRACT

Brain is a potential target for neuroprogestogens and/or peripheral progestogens. Previous studies reported that expression of genes about steroidogenesis, reproduction, cell cycle, and circadian rhythm in zebrafish brain could be affected by progestogens. However, there are limited information from metabolites or biomacromolecules aspects, leaving an enormous gap in understanding toxic effects of progestogens on fish brain. In this study, we exposed zebrafish embryos to 2.8, 27.6, and 289.8 ng/L dydrogesterone (DDG, a synthetic progestogen) until sexual maturity (140 days). LC-MS and GC-MS based untargeted metabolomics and Fourier-transform infrared (FTIR) spectroscopy were then performed to investigate the metabolic profiles and macromolecular changes of brain of these zebrafish. The results from multivariate statistical analysis of metabolite features showed a clear separation between different treatment groups of both female and male zebrafish brains. DDG exposure increased the levels of cholesterol, saturated fatty acids, and nucleoside monophosphates, but decreased the contents of polyunsaturated fatty acids (PUFAs), lysophosphatides, and nucleosides in dose-dependent manner. FTIR results indicated that DDG exposure led to accumulation of saturated lipids, reduction of nucleic acids and carbohydrates, and alteration of protein secondary structures. The findings from this study demonstrated that DDG could affect contents of metabolites and biomacromolecules of zebrafish brain, which may finally lead to brain dysfunctions.

1. Introduction

Endogenous progestogens are generally produced by gonad or adrenal gland. Besides, there are many synthetic progestogens used for human and animals. Dydrogesterone (DDG), a synthetic progestogen used for gynecological diseases and livestock breeding, was widely used in many countries (Fent, 2015). After use, its residues and metabolites may discharge into the receiving environment. As a result, DDG was found in various environmental media with concentrations ranging from 1.28 ng/L to 9330 ng/L (Liu et al., 2014; Liu et al., 2015; Yu et al., 2019; Zhang et al., 2021). DDG may also be converted from other progestogens in the environment, which is one of the reasons for its high environmental detection rate (Yu et al., 2019; Liu et al., 2020). Progestogens in the environment may pose a threat to wildlife, such as disrupting sex differentiation and reproduction of aquatic organisms. Previous studies have shown that DDG could disrupt expression of hormone-regulated genes, sex differentiation, gonad development, and reproduction of zebrafish (Zhao et al., 2015b; Shi et al., 2018; Jiang et al., 2019a; Jiang et al., 2019b; Shi et al., 2019).

Although progestogens are gonadal steroid hormone, their physiological effects extend well beyond the strict confines of reproductive functions. In fact, progestogens have important effects on a variety of tissues, including the bone, the heart and the brain. Progestogens can easily cross the blood–brain barrier and accumulate within the nervous

☆ This paper has been recommended for acceptance by Maria Cristina Fossi.

* Corresponding author.
E-mail address: wenjun.shi@m.scnu.edu.cn (W.-J. Shi).

https://doi.org/10.1016/j.envpol.2022.120811
Received 27 August 2022; Received in revised form 26 November 2022; Accepted 1 December 2022
Available online 2 December 2022

tissues, so they may affect various functions of the brain (Madigan et al., 2012). Brain possesses the enzymes necessary for production of neurosteroids either by synthesizing from cholesterol or metabolizing of progesterone and other steroids (Simoncini et al., 2007). Both nuclear and membrane progesterone receptors highly express and exhibit a very large distribution within the brain of zebrafish (Diotel et al., 2011). In addition to progesterone receptors, progestogens also work via the transmembrane γ-aminobutyric acid type A (GABAA) receptors to influence a wide variety of brain functions including neurogenesis, neuroprotection, neuroendocrine function, sexual behavior, sleep cycle, psychological function and behavioral function (Thomas and Pang, 2012; Leeangkoonsathian et al., 2017). Therefore, it is important to understand the effects of progestogens on brain of aquatic organisms such as fish.

Several recent studies reported that expression of genes along with the hypothalamic-pituitary-gonadal (HPG) axis, steroidogenesis, reproduction, cell cycle, and circadian rhythm in zebrafish brain could be affected after exposure to various progestogens, including DDG (Zucchi et al., 2013; Zucchi et al., 2014; Fent, 2015; Zhao et al., 2015b; Zhao et al., 2015a; Cano-Nicolau et al., 2016; Siegenthaler et al., 2017; Shi et al., 2018; Shi et al., 2019; Hou et al., 2020; Dong et al., 2022). Among all the pathways, only the circadian rhythm network showed prominent, dose-dependent and gender-consistent alterations, which was significant even at environmentally relevant concentrations of progestogens (Zucchi et al., 2013; Zucchi et al., 2014; Zhao et al., 2015b; Zhao et al., 2015a; Shi et al., 2018).

The concentration of DJ-1 chaperon protein was significantly increased in common roach brain by progestogens (progesterone, drospirenone, and levonorgestrel) (Maasz et al., 2017). Nuclear progesterone receptor knockout dominant zebrafish were significantly and persistently more aggressive with a robust dominance relationship (Carver et al., 2021). However, the effects of progestogens on fish brain have been still poorly studied from small molecule chemicals, biomacromolecules or behavioristics aspects, leaving an enormous gap in understanding toxic effects of progestogens.

Metabolites are small molecules that provide a functional readout of cellular state, so metabolite profiling helps to interrogate how mechanistic biochemistry relates to phenotype (Patti et al., 2012). Besides, with infrared spectroscopy, we can explore the alterations of structures and properties of biomolecules such as lipids, proteins, nucleic acids and carbohydrates at the biochemical levels (Martin et al., 2010). It is thus essential to combine metabolomics and infrared spectroscopy results with the existing transcriptomics data to fully understand the effects of progestogens on brain functions.

The objective of this study was to investigate the toxic effects of DDG on zebrafish brain by using metabolomics and biospectroscopy. Zebrafish embryos were exposed to different concentrations of DDG until sexual maturity. The brains were then dissected and used for analysis by metabolomics and Fourier transform infrared (FTIR) spectroscopy. The obtained results were further integrated with our previous transcriptomics data to have a better insight into the toxic mechanism of DDG on zebrafish brain.

2. Materials and methods

2.1. Materials

Dydrogesterone (DDG, CAS number: 152–62–5) was purchased from Dr. Ehrensorfer (Germany). Dimethylsulfoxide (DMSO) was used as the carrier (0.01%) for DDG. A detailed description of the methods is provided in the Supporting Information (SI Text S1).

2.2. Exposure of zebrafish to DDG

The parent zebrafish were obtained from a local supplier and acclimated for two months. At the beginning of the exposure, these zebrafish spawn and zygotes were collected. Five replicates constituted a treatment group. Each replicate contained about 190 zebrafish zygotes within 2 h post fertilization. At 35 days post-fertilization (dpf), some fish fry were removed leaving about 60 fish to continue the exposure until 140 dpf. DMSO with or without DDG was added to filtered and aerated tap water to form 0 (solvent control, C), 5 (L), 50 (M) and 500 (H) ng/L exposure solutions. The exposure system was semistatic and exposure solutions were renewed daily. Fish were kept in an environmental chamber with controlled temperature (27 ± 1.0 °C) and photoperiod (14 h light and 10 h dark).

The actual DDG concentrations in exposure solutions were confirmed during the experiment. To ensure water quality, the conductivity, pH, and dissolved oxygen concentrations were monitored every three days. Dead fish were recorded and discarded. At the end of the exposure, each zebrafish was anesthetized, body length and wet weight were measured, and the whole brain was dissected. The sampling time continued for approximately 4 h. All experiments were conducted with the approval of the Ethics Committee of South China Normal University for the Care and Use of Laboratory Animals (SCNU-ENV-2022-015).

2.3. Metabolomics method

The procedure for metabolomics analysis was the same as our previous publication (Jiang et al., 2019a). Briefly, brains of 20 females or 30 males from each replicate were snap-frozen in liquid nitrogen, pooled, freeze-dried, and stored at −80 °C waiting for metabolomics analysis. Smaller number of female zebrafish was investigated as DDG treatment has resulted in more male than female fish (Please refer also to SI Fig. S1). The prepared pooled-sample was transferred into 0.5 mL cold methanol solution (4:1 methanol: water, containing 20 μg/mL FMOC-glycine as internal standard) and 6–8 stainless steel beads were added. Then zebrafish brain samples were homogenized at 25 Hz for 10 min using a TissueLyser (QIAGEN, USA). The homogenate was sonicated for 10 min in ice water and centrifuged for 10 min at 12,000 rpm at 4 °C. One 100-μL aliquot of the supernatant was stored at −80 °C waiting for LC-MS analysis. Another 20 μL aliquot of the supernatant was used for derivatization using methoxylamine hydrochloride and MSTFA and the resulting mixture was used for GC-MS analysis.

Two platforms were used in the untargeted metabolomics analysis: Agilent 1290 ultra-high pressure liquid chromatography with 6540 quadrupole time-of-flight mass spectrometer (LC-Q-TOF/MS) and Agilent 7890 A gas chromatography with 7200 quadrupole time-of-flight mass spectrometer (GC-Q-TOF/MS). The column used was Zorbax SB-C18 column (1.1 × 50 mm, 1.8 μm, Agilent) and HP-5 MS UI column (30 m × 0.25 mm x 0.25 μm, Agilent), respectively. Both positive and negative modes were used in LC-Q-TOF/MS analysis with Milli-Q water and acetonitrile as the mobile phases and electrospray ionization (ESI) as ion source. At metabolites identification stage, targeted MS/MS analyses with collision energies at 10, 20 and 40 eV were conducted on the same condition as mentioned above.

Raw data acquired from LC-MS or GC-MS were converted to mzXML format and processed using XCMS Online (https://xcmsonline.scripps.edu) for peak picking, alignment, integration, and extraction of the peak intensities. The resulting three-dimensional data were further processed in Microsoft Excel for normalization and data filter. Then data were imported to SIMCA-P 14.0 (Umetrics, Umea, Sweden) for multivariate statistical analysis. Features with variable importance in the projection (VIP) score >1 in the orthogonal partial least squares-discriminant analysis (OPLS-DA) model were chosen to do Kruskal-Wallis test and then features with p-value <0.05 were selected for metabolite identification. The exact masses and MS/MS spectra of selected features from LC-MS were searched against the METLIN database (http://metlin.scripps.edu) and the HMDB database (http://www.hmdb.ca). The molecular features from GC-MS were identified by comparing the MS spectra with those in the NIST 11 library.

2.4. FTIR spectroscopy method

The procedure for FTIR analysis was based on our previous publication (Hu et al., 2017). At the end of the exposure, two adult male or female zebrafish were randomly selected from each tank (totally 5 tanks for each concentration) and their whole brains were dissected and fixed with 1 mL 10% (v/v) formalin overnight. Each fixed fish brain was washed 3 times with phosphate-buffered saline and water in sequence, then spread onto BaF_2 slides and dried in desiccator for at least 24 h. The prepared samples on BaF_2 slides were investigated using a Bruker Vector 70 FTIR spectrometer (Bruker Optics Ltd., UK) equipped with a Helios ATR attachment and a HYPERION microscope. Instrument parameters were 32 scans, and 16 cm^{-1} resolution. For each slide, 10 IR spectra were acquired at different points across the sample.

The data obtained in OPUS format were converted into TXT format and then imported into MATLAB r2010a (The MathWorks, Inc., US) for analysis using IRootLab toolbox (http://irootlab.googlecode.com). Data pre-processing was performed as follows: cut to 3050-2800 cm^{-1} (C–H stretching region) and 1800-900 cm^{-1} (the biochemical fingerprint range), rubberband baseline correction and normalization to Amide I peak (1650 cm^{-1}). These data could then be used for multivariate analysis. The spectra of each group could be averaged to obtain the average spectrum with or without centralization.

Principal component analysis (PCA) and linear discriminant analysis (LDA) were used here as multivariate analysis techniques. We applied PCA to capture most of the data information in a few factors which then served as input variables to be futher anayzed by LDA (PCA-LDA) (Martin et al., 2010). The results were visualized in the form of score plot and loading plot. In the score plot, nearness between two scatters indicates similarity, while distance means difference. The loading plot is composed of visualizing loadings vectors as wavenumber functions. Assignments of major peak wavenumbers are listed in Table S6.

2.5. Measurement of DDG concentration in exposure solution

The actual DDG concentrations in the fish culture water were determined at 6th, 30th, 70th, 100th and 130th day of exposure. Three replicates of water samples from all treatment groups were taken at the beginning (0 h) and end (24 h) of the selected exposure days. Samples were extracted by solid phase extraction on Waters Oasis HLB cartridges (200 mg, 6 mL). Analysis of DDG was performed on an Agilent 1200 series ultra-high-performance liquid chromatograph (Agilent, USA) coupled to an Agilent 6460 triple quadrupole mass spectrometer with electrospray ionization in positive ionization mode (UHPLC-ESI-MS-MS). The method limit of detection (LOD) was 0.08 ng/L, and the method limit of quantitation (LOQ) was 0.28 ng/L. The recoveries were 99 ± 5%. To obtain a mean concentration of DDG in each treatment condition during the exposure, the time-weighted mean concentrations were calculated according to annex 6 of the OECD TG 211 (OECD, 2012).

3. Results

3.1. Exposure solution quality and zebrafish conventional endpoints

The measured DDG concentrations at T_{24} of all the exposure groups decreased as fish growing up (SI Text S2). Therefore, the time-weighted mean concentrations of DDG in the C, L, M, and H treatment group were 0, 2.8, 27.6, and 289.8 ng/L, respectively (SI Table S1), which were presented as actual concentrations. There were no significant differences in the pH, conductivity, and dissolved oxygen concentration of the exposure solutions between the control and exposure groups (SI Table S2).

During the exposure, DDG did not elicit appreciable difference in behavior and mortality rates between the exposed and control groups (SI Table S2). However, DDG led to marked male-biased zebrafish sex ratios, resulting in no female fish samples available from the H group for the metabolomics and FTIR studies, as 98% zebrafish developed into male (Jiang et al., 2019b).

3.2. Metabolite profiles of zebrafish brain

Metabolite ion features from the three analytical procedures after data preprocessing were used for multivariate statistical analysis. An unsupervised principal component analysis (PCA) model was constructed to examine intrinsic clusters of global metabolites of each treatment. To provide a better separation according to classification of the samples, a supervised orthogonal projection to latent structure-discriminant analysis (OPLS-DA) was used. Clear separation between different treatment groups was observed on both the PCA and OPLS-DA score plots of female zebrafish (Fig. 1). As shown in the PCA and OPLS-DA score plots of male zebrafish, the metabolic profile of the control group was clearly discriminated from the exposure groups, and noticeable separation was observed between the high exposure (H) group and the other exposure groups (Fig. 1). The reproducibility of the method had been checked with the performance of QC samples, thus the differences in metabolic profiles reflected compositional differences between different treatments.

Features that contributed to the discrimination of each group, namely VIP >1 and $p < 0.05$, were selected as key metabolites to be identified. Finally, 61 significant metabolites were identified, and their differences within the data set are shown using ion feature abundances (Table 1). Overall, these metabolites belong to monoglycerides, steroids, fatty acids, lysophosphatides, nucleosides, nucleotide sugars, sugars, amino acids, acylcarnitines, and organic acids. The full name and other detailed information of these identified metabolites are listed in SI Tables S3-S5.

The performances of many identified metabolites were similar for both female and male zebrafish brains (Table 1). The relative concentration of monoglycerides increased after exposure to DDG. Similarly, cholesterol and saturated fatty acids (SFAs), namely myristic acid, palmitic acid, and stearic acid, increased by DDG in a dose-dependent manner (Fig. 2). On the contrary, the levels of unsaturated fatty acids, especially those polyunsaturated fatty acids (PUFAs) such as arachidonic acid (AA), α-linolenic acid, stearidonic acid, eicosapentaenoic acid (EPA), decosahexaenoic acid (DHA), and their hydroxyl metabolites decreased as DDG concentration increased. In agreement with the variation trend of PUFAs, the contents of lysophosphatides, mainly lysophosphatidylthanolamines (LPE), were low in the DDG exposure groups. As for nucleosides and their bases, such as inosine and hypoxanthine, decreased in abundance, while nucleoside monophosphates such as AMP, GMP, and UMP increased after DDG exposure in both female and male zebrafish brains (Table 1).

However, disturbances of the production of some other metabolites showed differential patterns of variation in female and male zebrafish brains. Sugars, including UDP-sugars, glucose, and gluconate 6-phosphate, were increased in female brain but decreased in male brain by DDG (Table 1). In contrast, many metabolites belonging to amino acids, acylcarnitines, and acyltaurines were decreased in female brain while increased in male brain by DDG. In addition, productions of organic acids such as citric acid, malic acid, and fumaric acid were also affected after DDG exposure (Table 1).

3.3. Biochemical effects based on FTIR

After 140 days of DDG exposure, brain of zebrafish was dissected for infrared spectroscopy analysis. In female brains, from the average spectrum (Fig. 3A) and PCA-LDA score plot (Fig. 3B), it can be seen that there are differences among treatment groups. According to the PCA-LDA loading plot (Fig. 3C) and the average spectrum obtained after centralized processing (Fig. 3D), DDG exposure increased the lipid-related absorptions in the brain of female fish, such as the 3050–2800

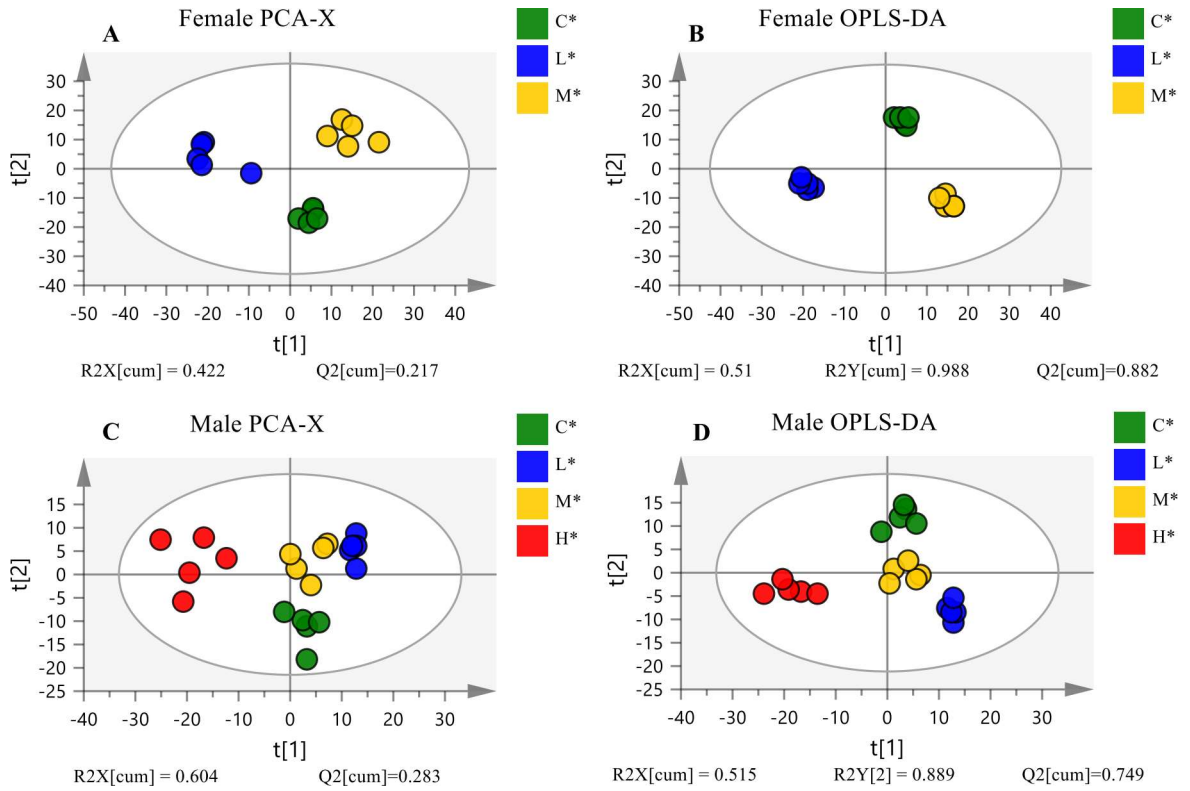

Fig. 1. Multivariate statistical analysis of metabolite profiles of zebrafish brain after 140 days of dydrogesterone exposure. PCA and OPLS-DA score plots of female (A and B) and male (C and D) zebrafish brain show clear separation between different groups. The missing of female data in H group is due to insufficient females for investigation. Each dot represents one replicate. Abbreviations: C, solvent control; L, low dose; M, medium dose; H, high dose.

cm^{-1} region where the spectrum is due to absorptions from the C–H stretching vibrations of olefinic CH, CH_2 and CH_3 groups, 1469–1450 cm^{-1} which can be attributed to bending vibration of the CH_2 and band at 1743 cm^{-1} originates from fatty acid ester C═O (Table S6). When the relative sizes of the above bands were further analyzed, it was found that saturated lipids (2923 cm^{-1}) and oxidized lipids (1747 cm^{-1}) were increased while unsaturated lipids (3012 cm^{-1}) were decreased by DDG (Table 2). Absorption variation of these bands suggested that exposure to DDG led to accumulation of lipids in the brain of female fish, particularly the saturated lipids.

In contrast to lipids, DDG exposure resulted in a significant reduction of nucleic acids related absorptions at 1709 cm^{-1}, 1585 cm^{-1}, 1226 cm^{-1}, 1084 cm^{-1}, and carbohydrate related absorption at 1030 cm^{-1} in female brain (Fig. 3D, Table S6). Besides, DDG exposure also affected the secondary structure of proteins in female brain as indicated by the shift of Amide I peak (1628 cm^{-1} to 1670-1655 cm^{-1}).

As for the male brain, both average spectrum (Fig. 3E) and PCA-LDA score plot (Fig. 3F) showed that the H group was clearly different from other treatment groups. From the PCA-LDA loading plot (Fig. 3G) and the centralized average spectrum (Fig. 3H), it can be seen that the effects of DDG on lipids in male brain were puzzling. DDG resulted in a significant reduction in the absorption of the C–H stretching (3050-2800 cm^{-1}) in the exposure group. However, other lipid-related absorption peaks increased in the exposure groups, such as fatty acid ester C═O stretching (1747 cm^{-1}), CH_2 antisymmetric bending (1458 cm^{-1}), lipid COO- stretching (1408 cm^{-1}), and CH_3 antisymmetric bending (1369 cm^{-1}) (Fig. 3H). When considering the biomarkers of lipids, both lipid saturation and lipid oxidation increased due to DDG exposure (Table 2).

Absorption peaks associated with nucleic acids at 1585 cm^{-1}, 1211 cm^{-1}, 1072 cm^{-1}, and absorption peak of carbohydrate at 1045 cm^{-1} were significantly reduced by DDG in male brain (Fig. 3H). Besides, DDG exposure altered the secondary structure of the protein by increasing the amount of protein with antiparallel β-sheet conformations (1685 cm^{-1}).

4. Discussion

In this study, the combined LC-MS and GC-MS based metabolomics and Fourier transform infrared (FTIR) spectroscopy were for the first time applied to investigate the effects of DDG on zebrafish brain following exposure of zebrafish embryos to different concentrations of DDG for 140 days. Both metabolite profiles and FTIR spectra of treated and control zebrafish brain showed marked differences with each other, indicating metabolic and biomacromolecular disturbances induced by DDG.

In both female and male, DDG exposure increased the levels of monoglycerides, cholesterol, and saturated fatty acids, while decreased the contents of PUFAs and lysophosphatides (Table 1). All of these metabolites are components of lipids, in particular phospholipids (Huang and Freter, 2015). Similarly, DDG exposure increased the intensity of all the lipid-related bands in female brain and many of the lipid-related absorption peaks in male brain, such as 1747 cm^{-1}, 1458 cm^{-1}, 1408 cm^{-1}, and 1369 cm^{-1} (Fig. 3). These peaks were attributed to neutral lipids, sphingolipids and phospholipids (Dreissig et al., 2009). Thus the increased intensity of these bands indicated more lipids accumulation in DDG treated zebrafish brain. Moreover, DDG increased lipid saturation and lipid oxidation in both female and male zebrafish brain as suggested by relative FTIR absorption peak magnitudes between saturated lipids (2923 cm^{-1}), unsaturated lipids (3012 cm^{-1}), and oxidized lipids (1747 cm^{-1}) (Table 2) (Mignolet et al., 2017). According to both metabolic profiles and FTIR results, we believe that DDG exposure disrupted lipid metabolism, and finally led to accumulation of saturated lipids and reduction of unsaturated fatty acids in zebrafish brain.

To our knowledge, few studies have explored the changes of lipids in fish brain after exposure to progestogens. In human neuroblastoma cells, the addition of progesterone to the linolenic acid enriched medium decreased by 9% the mRNA expression of the Δ6-desaturase, a key gene of PUFA conversion (Extier et al., 2009). In rats, contents of brain DHA

Table 1
Relative abundances of identified metabolites in zebrafish brain following 140 days of dydrogesterone exposure[a].

Compound	Relative ion intensity							P values					Class
	F-C	F-L	F-M	M-C	M-L	M-M	M-H	F-L	F-M	M-L	M-M	M-H	
MG(16:0/0:0/0:0)	83508	102078	109735	85416	90753	98645	105681	**0.026**	**0.027**	0.112	**0.010**	**0.013**	Monoglycerides
MG(18:0/0:0/0:0)	438180	601666	772717	543308	515507	550967	643265	**0.000**	**0.004**	0.486	0.803	0.121	
Cholesterol	226499	222526	433221	120768	147924	151116	189702	0.818	**0.002**	**0.043**	0.062	**0.001**	Steroids
Myristic acid	26112	29818	39942	19587	24863	24878	28051	0.333	**0.000**	**0.017**	**0.003**	**0.002**	Fatty acids
Palmitic acid	919009	1046010	1365671	767292	792483	1030324	1101147	0.172	**0.001**	0.727	**0.019**	**0.005**	
Stearic acid	230834	259078	318441	208697	229054	235776	270765	0.371	**0.001**	0.155	0.169	**0.006**	
Octenoic acid	2823073	3128219	3320613	3263051	3138850	3244647	3362599	**0.024**	**0.004**	0.423	0.885	0.615	
Palmitoleic acid	5103548	4733189	6018717	4144088	3512506	3237398	2995404	0.290	0.144	0.055	**0.007**	**0.003**	
Oleic acid	471413	250652	310870	332463	382529	279131	211962	**0.001**	0.069	0.218	0.115	**0.007**	
16-hydroxy hexadecanoic acid	25150	20095	13212	13026	12732	9258	6969	0.094	**0.001**	0.901	0.170	**0.018**	
9,10-Epoxystearic acid	109396	87485	59226	86337	94459	65087	53193	**0.048**	**0.001**	0.421	0.073	**0.009**	
Linoleic acid	24220	13904	12330	24088	21624	19860	16257	**0.000**	**0.001**	0.343	0.079	**0.026**	
Eicosatetraynoic acid	42019	20198	24653	42751	20672	29499	16831	**0.008**	**0.019**	**0.001**	**0.044**	**0.000**	n-6 PUFAs
AA	7478	2123	1513	2354	2168	1685	561	**0.000**	**0.000**	0.534	0.081	**0.003**	
9-HODE	21342	19962	11510	23183	16198	18018	12165	0.632	**0.004**	0.096	0.292	**0.017**	
5-HETrE	32664	12641	13616	11777	5106	7734	6146	**0.004**	**0.004**	**0.005**	0.056	**0.012**	
5-HETE	943632	424273	362351	486295	230471	334085	204953	**0.006**	**0.003**	**0.001**	**0.018**	**0.000**	
5-oxo-ETE	85074	46915	34508	45179	31549	34152	18146	**0.005**	**0.001**	0.081	0.185	**0.003**	
5-HETE lactone	101212	44963	43488	47480	26966	35915	20945	**0.009**	**0.007**	**0.001**	**0.002**	**0.000**	
α-Linolenic acid	13867018	11151112	9454555	9966170	8915926	7722999	6978110	0.056	**0.008**	0.290	**0.038**	**0.024**	n-3 PUFAs
Stearidonic acid	4743335	3550086	2845456	4022261	3319420	2810158	2148111	**0.030**	**0.005**	0.162	**0.027**	**0.006**	
EPA	162068	73069	63904	82900	40862	60484	37025	**0.005**	**0.003**	**0.000**	**0.040**	**0.000**	
DPA	2796122	2341810	2282114	2080467	1678867	1657983	1372106	0.156	**0.024**	0.062	0.055	**0.011**	
DHA	69912	45633	45839	55391	38779	40266	21851	**0.003**	**0.013**	0.084	0.074	**0.001**	
5-HEPE	217010	96714	110911	181242	86757	99630	61401	**0.004**	**0.009**	**0.000**	**0.000**	**0.000**	
18-HEPE	4575	3258	2899	7082	4726	5512	3306	**0.010**	**0.001**	**0.021**	0.112	**0.001**	

(22:6 n-3) and two other PUFAs (20:2 n-6 and 22:5 n-3) decreased after pregnancy (high progesterone concentration period) (Levant et al., 2006). In mice, diets containing different concentrations of PUFAs greatly modified total fatty acids, sphingolipids, and gangliosides in the cerebral cortex, which was dependent on ovarian hormones, including progesterone (Herrera et al., 2018). Our study indicated that long-term exposure to progestogens perturbed lipid metabolism in zebrafish brain, which might break the subtle balance between saturated and unsaturated fatty acids and finally disrupt normal functions of zebrafish brain.

Phospholipids, major components of neural cell membranes, participate in synaptic transmission and neuronal signaling through interactions with specific membrane proteins (Bazan, 2014). PUFAs are the major structural and functional components in nerve cell membrane phospholipids. The deficiency of n-3 PUFAs has been shown associating with schizophrenia, depression and other mood disorders, attention deficit, hyperactivity disorder, post-traumatic stress disorder, and Alzheimer-type dementia in humans (Yonezawa et al., 2020). On the contrary, saturated free fatty acids, including stearic acid, lauric acid, and palmitic acid, are closely associated with neurodegenerative processes such as dementia, stroke, epilepsy, spinal cord injury, Parkinson's disease, neuroinflammation, and Alzheimer's disease (Osorio et al., 2020).

In particular, some metabolites can lead to circadian disruption. Saturated fatty acids have earlier been shown implicating in circadian clock disturbance (Blancas-Velazquez et al., 2017). High fat diets that are rich in saturated lipids altered the normal rhythm of locomotor activity, feeding, sleep and core clock gene mRNA expressions, such as *Bmal1*, *Per2* and *Rorα*, in rats and mice (Kohsaka et al., 2007; Greco et al., 2014). High-fat and high-cholesterol diet significantly increased the expression of *Bmal1* but decreased the expression level of *Per2* and *Per3* in rats, which were rescued by fish oil that is rich in n-3 PUFAs (Yuan et al., 2016). Similarly, palmitate exposure caused dysregulation of both *Bmal1* and *Rev-erbα*, while DHA repressed these palmitate-induced phase shifts of the mHypoE-37 neurons or fibroblast clock (Greco et al., 2014; Kim et al., 2016). Moreover, n-3 PUFAs-deficient diet has been shown to lessen the melatonin rhythm, disturb nocturnal sleep, and weaken endogenous functioning of the circadian clock in hamsters (Lavialle et al., 2008).

Effects of progestogens on zebrafish brain, including DDG, have been investigated, mainly from transcriptional aspect, indicating that circadian rhythm was the most significant pathway that could be disturbed (Zucchi et al., 2013; Zucchi et al., 2014; Zhao et al., 2015b; Zhao et al., 2015a; Shi et al., 2018). Thus we speculate that the disturbance of biomolecules induced by DDG may disturb circadian clock of zebrafish. To explore this issue, correlation matrixes were used to evaluate the interdependence of metabolites from the present study and circadian clock genes from our previous study (Shi et al., 2018), using Pearson's correlation tests. The correlation matrices between the metabolites and circadian clock genes from the microarray and qPCR of male and female are noteworthy and basically the same (SI Table S7-S9), suggesting that circadian rhythm is a genderless and vulnerable target of DDG. Therefore, DDG might disrupt zebrafish circadian rhythm *via* increasing the level of saturated lipids, such as palmitic acid and cholesterol, and decreasing the level of n-3 PUFAs, especially DHA, as supported by our metabolomics and FTIR results (Figs. 2 and 3).

Besides, DDG led to alterations in metabolic profling of amino acids (Table 1), indicating disturbance of amino acid metabolism, which might contribute to the alteration of protein secondary structure as shown by the FTIR absorption (Fig. 3). Previous studies have shown dietary PUFA modified the expression of neuronal proteins such as

Compound	Relative ion intensity							P values					Class
	F-C	F-L	F-M	M-C	M-L	M-M	M-H	F-L	F-M	M-L	M-M	M-H	
7-HDoHE	1273490	535947	564053	873693	419487	571002	362192	**0.003**	**0.004**	**0.001**	**0.006**	**0.000**	
20-HDoHE	29526	20897	22727	35026	25079	27294	20493	0.090	0.121	0.154	0.208	**0.019**	
Arachidonoyl glycidol	63159	25070	26402	21641	23744	18808	17359	**0.000**	**0.000**	0.276	0.206	**0.045**	
LPC(14:0/0:0)	213240	77468	68900	100239	108120	81387	62144	**0.024**	**0.018**	0.542	0.143	**0.008**	
LPE(16:0/0:0)	357904	281269	282103	415200	362922	344352	279418	**0.003**	**0.001**	0.165	0.143	**0.004**	
LPE(16:1(9Z)/0:0)	39443	31811	26606	53109	59436	49496	24315	0.175	**0.027**	0.477	0.667	**0.000**	Lysophosphatides
LPE(17:0/0:0)	28728	19546	20469	26989	23957	25772	20222	**0.021**	**0.010**	0.427	0.786	0.087	
LPE(18:1(9Z)/0:0)	283893	157190	94539	139918	198700	146551	91304	**0.001**	**0.000**	**0.028**	0.784	**0.016**	
LPG(16:0/0:0)	14923	7592	6136	11538	12771	9844	7740	0.065	**0.031**	0.342	0.235	**0.013**	
Hypoxanthine	234284	203309	101666	292622	187933	158882	133379	**0.043**	**0.000**	**0.000**	**0.000**	**0.000**	
Inosine	146278	135918	104071	162935	137402	145439	126721	0.276	**0.005**	**0.041**	0.183	**0.009**	
Guanine	171091	157904	115218	167922	158313	134284	121807	0.112	**0.000**	0.225	**0.002**	**0.001**	
Uracil	110883	107395	67443	126584	92472	93406	86853	0.685	**0.001**	**0.001**	**0.001**	**0.002**	Nucleosides
IMP	56902	66470	114399	41055	66456	77436	83294	0.207	**0.000**	**0.002**	**0.000**	**0.000**	
AMP	36614	36908	94626	22571	55956	66454	98115	0.944	**0.000**	**0.000**	**0.000**	**0.000**	
GMP	11767	14682	27614	10181	19226	20138	22291	0.057	**0.000**	**0.000**	**0.000**	**0.000**	
UMP	3889	7488	15923	3691	6412	7328	8253	**0.001**	**0.000**	**0.003**	**0.000**	**0.000**	
UDP-glucose	41477	49567	71739	57489	54950	55424	53923	**0.044**	**0.000**	0.389	0.444	0.139	
UDP-glucuronic acid	8165	25129	16680	11939	11895	13224	11628	**0.000**	**0.000**	0.955	0.221	0.676	Nucleotide sugars
UDP-N-acetylglucosamine	98371	133800	222062	138736	128477	129458	120428	**0.000**	**0.000**	0.187	0.232	**0.021**	
Glucose	61783	1464387	193502	79193	187708	275669	76989	**0.001**	**0.004**	**0.033**	**0.004**	0.862	Sugars
Glucose 6-phosphate	40585	44232	51420	44786	50836	42556	31438	0.066	**0.001**	**0.004**	0.337	**0.000**	
Pantothenic acid	28264	25266	32361	20783	20637	19486	16486	0.263	0.181	0.907	0.228	**0.002**	Vitamins
L-Aspartic acid	494871	415132	348913	378386	480238	442781	524288	**0.042**	**0.002**	**0.016**	**0.025**	**0.035**	
L-Glutamic acid	2118536	2036658	1788331	1858708	2353782	2075829	2544038	0.632	0.060	**0.007**	0.210	0.055	Amino acids
Glutathione, oxidized	47369	53864	55826	61523	51308	77889	105612	0.137	0.142	0.134	**0.028**	**0.001**	
Dodecanoylcarnitine	49161	39837	41431	39504	32167	45918	59330	**0.000**	**0.000**	**0.005**	0.132	**0.009**	Acylcarnitines
Myristoylcarnitine	187237	149413	140635	197221	127365	248614	319279	**0.025**	**0.004**	**0.003**	0.096	**0.010**	
Palmitoyl taurine	59195	52968	50999	57519	64311	70327	73733	0.197	**0.033**	**0.026**	**0.005**	**0.035**	Acyltaurines
Compound	Relative ion intensity							P values					Class
	F-C	F-L	F-M	M-C	M-L	M-M	M-H	F-L	F-M	M-L	M-M	M-H	
Oleoyl taurine	30327	23774	20452	24887	26648	28937	33088	**0.003**	**0.000**	0.488	0.113	**0.001**	
Arachidonoyl taurine	22841	18575	19573	20458	11907	18288	30451	0.110	0.163	**0.000**	0.101	**0.000**	
Lactic acid	30877944	30169118	35009487	41880891	38971444	43766937	43284354	0.742	0.190	0.414	0.635	0.659	
Citric acid	8294	8538	7372	8719	7215	11700	15065	0.847	0.497	0.115	**0.034**	**0.004**	Organic acids
Malic acid	672306	486861	509634	580689	762625	684874	611772	**0.002**	**0.010**	**0.016**	0.090	0.576	
Fumaric acid	77077	50024	54876	67673	70990	65941	59713	**0.000**	**0.000**	0.452	0.690	0.144	

[a] Detail information of the metabolites are provided at SI Table S3-S5. The abundance of each metabolite is mean ion intensity of five replicates from each treatment condition. The table cell colors, created by Excel Conditional Format, show the relative abundance of each metabolite in female or male brain samples, the darker the larger. *P* value < 0.05 (from Student's T test, in bold) represents significant difference comparing to the control group. The data of H group female are missing due to sample lacking. Abbreviations: C, solvent control; L, low dose; M, medium dose; H, high dose; F, female; M, male.